Defect Automatic Detection for Tire X-ray Images using Inverse Transformation of Principal Component Residual

XueHong Cui[1,*] , Yun Liu[1] and ChuanXu Wang[1]

[1] *School of Information Science and Technology*

Qingdao University of Science and Technology, Qingdao, Shandong, China
cuixuehongzhe@163.com

***Abstract*—We develop an image reconstruction algorithm in this paper using inverse transformation of principal component residual to automatically detect the tire defects in its X-ray image. A tire X-ray image to be inspected is first transformed to a new coordinate system, i.e. principal component space, in which the k major components and their corresponding eigenvectors represent the dominant normal textures of tires; Unlike traditional principal component analysis, we set the k major component eigenvalues as zeros, then the above principal component space matrix is called principal component residual in this paper, which stands for none-dominant textures of tires that is considered as abnormal or defect textures. We perform inverse transformation of this principal component residual and reconstruct the defect left only image. To localize the defect part, binarization operation is processed on the obtained left over image with upper and lower thresholds statistically. The proposed scheme can both reveal the defect locations and also present defect patch shapes for identifications. The experiment results show the high effectiveness of our scheme in detecting defects for tire X-ray images.**

Keyword: Tire X-ray image; Defect detection; Inverse Transformation ; Principal Component Residual

1. INTRODUCTION

With the rapid development in car industry, aerospace and aviation, the nondestructive defects detection and quality evaluation for tires have become significant steps in the industrial production. These detection technologies for tires mainly are based on laser, X-ray, ultrasound, electrical pulse and electromagnetic wave technology [1,2]. Especially in [1], the method based on X-ray began to be recognized by the academic community and it is very valuable in industrial production for giving assistance or replacing repetitive and subjective manual visual inspection processes. Therefore, this type of non-destructive detection technology is used widely in automated industrial defect inspection systems.

The defect detection algorithms for X-ray images are carried out both in spatial and frequency domains, while spatial computations cost more time and hardly in real time. Frequency based methods raise more concerns, these frequency based algorithms mainly include image component decomposition [4], dictionary-based Method [5,6,7], independent component analysis [8,9], singular value decomposition [10,11], and discrete Fourier transform [12], discrete wavelet transform [13,14]. All of them have higher precision and higher computational speeds for defect detection of periodic textured images.

The PCA method is widely applied in many fields successfully. PCA applications in computer vision include image representation, face recognition as well as image compression, etc. In this paper, we propose a new scheme which based on the principal component analysis (PCA) for tire defect detection. Unlike traditional PCA methods, rather than using X-ray image principal components, we

exploit its least significant components instead and isolate its defect texture patches if any in tires. The rest parts of this paper is organized as followings. We propose the whole algorithm of tire defect detection in section 2, and in section 3, we discuss our experiments and experimental results, finally, some conclusions are given in section 4.

2. TIRE DEFECT DETECTION SCHEME

2.1. Principal components and their corresponding textures in X-ray image

PCA is mathematically defined[15] as an orthogonal linear transformation that converts thedata into a newcoordinate system such that the greatest variance by some projection of the data comes to lie on the first coordinate (called the first principal component), the second greatest variance on the second coordinate, and so on.The first principal component hold as much of the variability in the data as possible, and each subsequent component accounts for as much of the remaining variability as possible. For a periodic textured tires X-ray image, the larger eigenvalue it has, the more texture information it contains. The main information of an image can be well approximated by the major k principal components and the corresponding eigenvectors. All other smaller principal components and the corresponding eigenvectors represent the local defects information if they are innate inside tire image.

For an $n\times m$ image X , following paper [16] ,we partition the input image into a set of n row vectors, $X=[x_1,x_2,\cdots,x_n]^T$. Accordingly, it can also be considered to be a set of m column vectors, Center the image X by subtracting column mean vector m_X . The PCA is performed for an image data X , and the new data Y after dimension reduction are obtained: $Y=W(X-m_X)$, where $Y=[y_1,y_2,\cdots,y_k]^T$ is a set of row vectors of K uncorrelated principal components; $W=[w_{ij}]_{k\times k}$ is a set of k-dimensional vectors, where w_{ij} stands for the j^{th} variable for i^{th} principal component whose columns are the eigenvectors of covariance matrix $(X-m_X)^T(X-m_X)$ and are orthonormal. Firstly, we get the W by computing the eigenvectors of covariance matrix $(X-m_X)^T(X-m_X)$ and rank them descendingly with eigenvalues. The principal components are given in order of significance.

2.2. Defect isolation based on inverse transform- ation of principal component residual

Given an $n\times m$ image X , the whole algorithm is shown in Fig.1, which is called inverse transformation of principal component residual (ITPCR). Some further information should be needed to explain below.

Step 1: the first basic pre-processing is image centering in first block as $X-m_X$, where $m_X=(1/m)\times(x_1+x_2+\cdots+x_m)$ is column mean vector, covariance matrix of X is calculated as $(X-m_X)^T(X-m_X)$.

Step2: Calculate the covariance matrix $(X-m_X)^T(X-m_X)$ of data X .

Step 3: Eigenvalue decomposition of covariance matrix. The eigenvecors of the covariance matrix corresponding to the greatest eigenvalue is the first principal component, in turn, the eigenvectors of the covariance matrix corresponding to the second greatest eigenvalue is the second principal component, and so on.

Step 4: Select the major k eigenvalues and set them to zeros, then get $\tilde{W}^{\mathrm{T}}$, parameter k will be discussed in next subsection.

Step 5: Reconstruct original image $\tilde{X}$ with inverse transformation of principal component residual.

$$\tilde{X}=\tilde{W}^{\mathrm{T}}\tilde{Y}+m_X=\sum_{j=1}^{K}\tilde{W}_j^{\mathrm{T}}\tilde{y}_j+m_X,j=1,2,\cdots,k \quad (1)$$

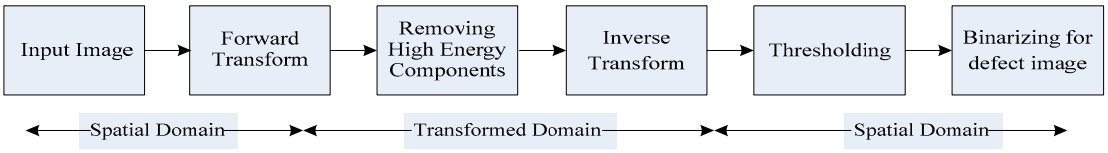

Fig.1 Global approach for defects Detection

Step 6: Obtain binarized image for defect isolation. Perform binarization on the reconstructed image $\tilde{X}$ using statistically controlled upper and lower thresholds for outstanding defect patches isolation. Binarization is given as:

$$\tilde{f}(x,y)=\begin{cases}255 & if \quad \mu-c\cdot\sigma\le\hat{X}\le\mu+c\cdot\sigma\\ 0 & otherwise\end{cases} \tag{2}$$

here c is a control coefficients constant, and σ and μ are the standard deviation and mean respectively of $\tilde{X}$, choice of these threshold values will be tested later on.

2.3. Selecting the right number of principal components

How to determine a proper k eignvalues is a key issue which is of great impact on the detection effectiveness of tire defects. We displayed the influences of different k values on restructuring capability for defect tire image. Fig. 2a was an original tire sidewall image with the foreign matter defects. Fig. 2a was transformed into principal component space and then reconstructed it by selecting different k values. Let k=1, the texture of Fig. 2a was not well reconstructed, and only horizontal linear textures were reconstructed which was shown in Fig. 2b. This phenomenon in Fig. 2b is the cause of underspecification of less k and leads to a loss of texture information in the reconstructed image. Let k=2,3, the textures were reconstructed relatively well which were shown in Fig. 2c-d. However, with the increasing of k values, the reconstructed image demonstrated increasingly significant the foreign matter defects which was shown in Fig. 2e–j. These phenomena are caused by overspecification of k values. As can be seen in Fig. 2b–j, under- or over-specification of the k values will cause the reconstructed image to deviate the normal structure contents.

We follow the Scree Graph and the Log-Eigenvalue Diagram to chose the best k. In our experiments, As can be seen in Fig.3, Log-Eigenvalues are ranked with descending order, the former three components are all larger than one, thus the former three principal components and the corresponding eigenvectors should contain dominant normal texture information. Fig.4 displays the reconstructed image based on inverse transformation of principal component residual with k=3, which looks dark and contains low image energies left. As can be seen that the dominant normal texture information has been removed away and the left local foreign matter defect are retained.

2.4. Statistically controlled binarization method

Because pixel gray-levels in above residual image $\hat{X}$ (as shown in Fig.4) are only slightly different. the statistical process control binarization method is adopted to set the upper and lower thresholds for outstanding the tire defects. This method is given as follows:

$$\tilde{f}(x,y)=\begin{cases}255 & if \quad \mu-c\cdot\sigma\le\hat{X}\le\mu+c\cdot\sigma\\ 0 & otherwise\end{cases}$$

here c is a control coefficients constant, and σ and μ are the standard deviation and mean respectively of $\hat{X}$. If a pixel gray level falls between the upper and the lower thresholds, its value is set to 255 and regarded as a non-defective texture element of tire to be removed; otherwise, its value is set to 0 and regarded as a defective element of tire to be retained. Fig.5 displays the binarized result image of Fig.4 for c=4.5, which clearly shows white non-defective texture area and dark defective patches, in the following experiment part we will talk about its statistical value of parameter c.

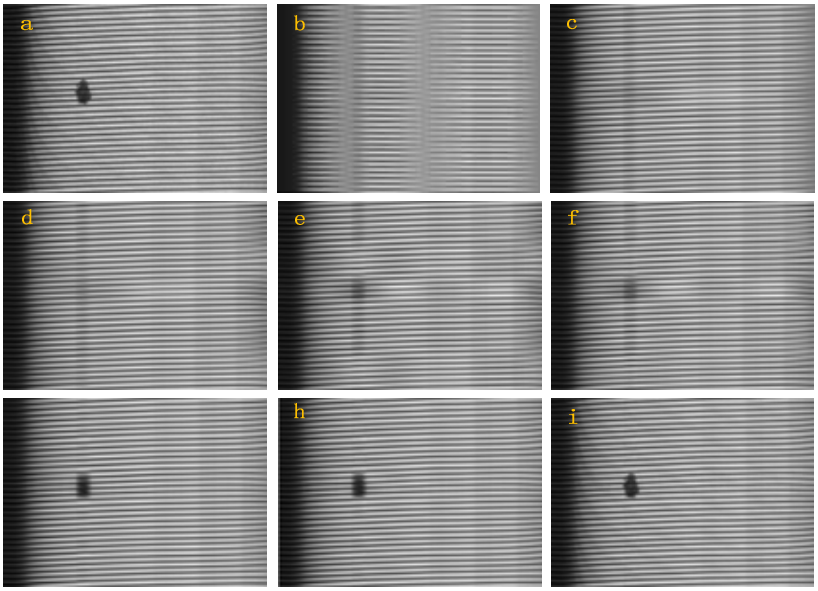

Fig. 2 Comparison of reconstructions with different k principal components. (a)tire sidewall X-ray images with the foreign matter defect.(b)–(j) reconstructed images from different k principal components as k=1,2,3,4,5,7,12,15

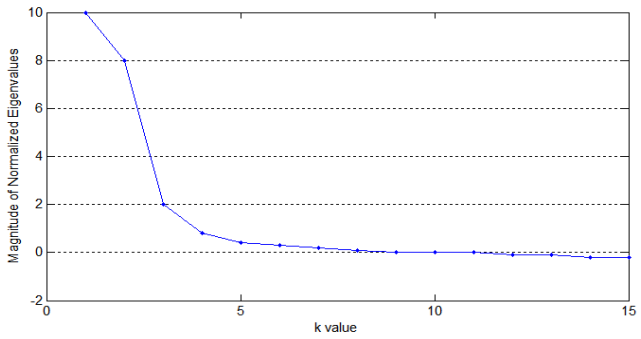

Fig. 3 The first fifteen largest normalized eigenvalues of Fig. 2a.

3. EXPERIMENT RESULTS AND ANALYSES

3.1 Experiment initialization

We carry out the presented scheme and evaluate its performances on various tire defects detection. Our proposed scheme is performed on Intel Core 2 Quad core processor Q9400 2.66GHz with 4 GB RAM and under MATLAB R2009b. Due to the tire X-ray image with multi-texture characteristics, it brings a great challenge for defect detection. Therefore, we need to first divide the tire X-ray image into four regions, which are the crown, the shoulder, the sidewall and the circle region. Therefore, we typically focus on tire X-ray images of different areas with defective or non-defective samples, including tire sidewall X-ray images with the foreign matter defect, with the bubble defect, with non-defect; also tire crown X-ray images with foreign matter defect and with non-defect.

3.2 Tests on sidewall region defect isolation

(1) Choice of statistical value of parameter c

We determine the value of parameter c for our proposed scheme with 15 learning images, which are composed of 8 defective samples and 7 defect-free samples. The number of correct detections were recorded as parameter c varied from 0.5 to10.0 at increment of 0.5. The value of parameter c was selected atits highest correct detection rate. That is, the c=4.5 is optimum for tire sidewall region.

(2) Performance validation for sidewall region defect isolation

Fourtest example images areshown in Fig.6 (a1)–(a4) with parameter settings of k=3 and c=4,which are one defect-free and three different defects innate to sidewall region. Fig.6 (b1)–(b4) display the correspondingreconstructed imagesbased on ITPCRwith k=3, which only took less than 0.20 second in average for each image operation. Fig.6 (c1)–(c4) display the accompanying binarized images with threshold of c= 4.5.

As you can see, Fig.6 (c1) does not show any defects inside, and Figs.6 (c2)–(c4) display clearly the defects which are originally contained in tire.

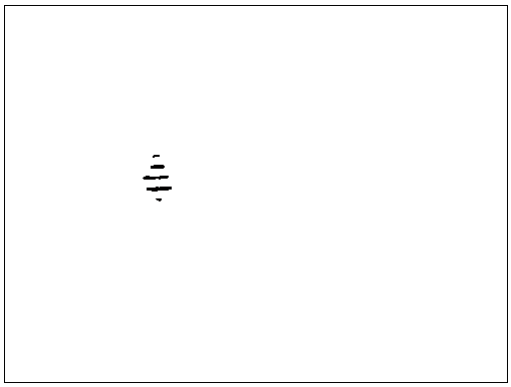

Fig.4 Reconstructed image based on ITPCRwith k=3 Fig.5 binarization mask image of Fig. 4

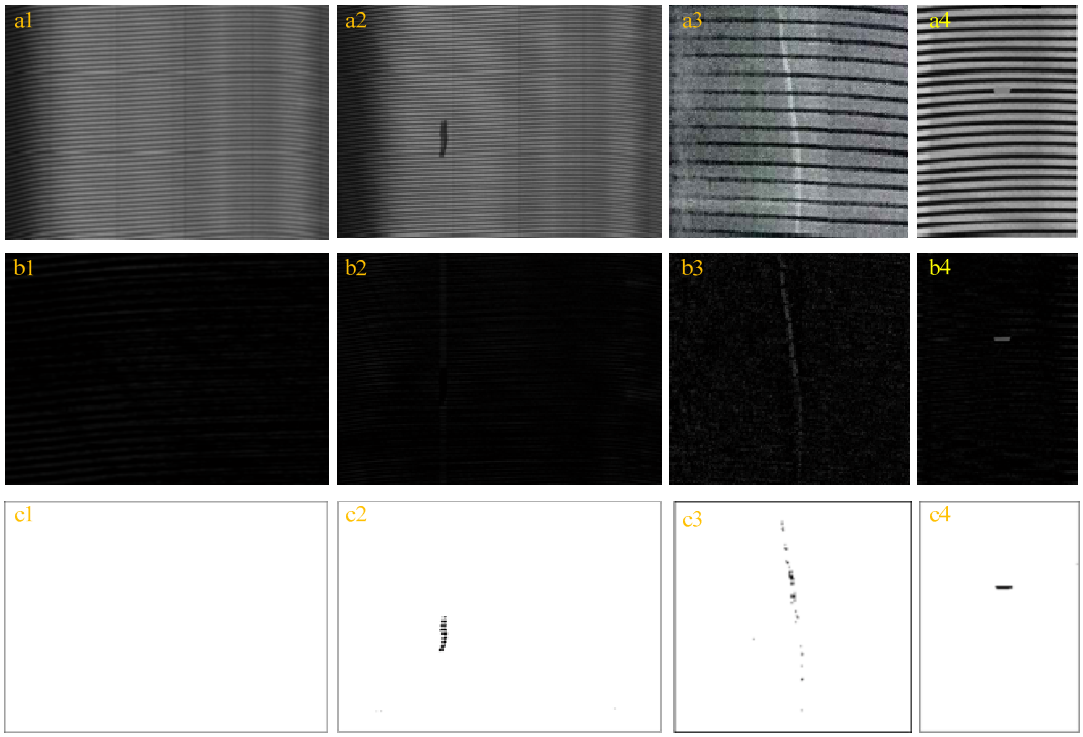

Fig. 6 Tests on sidewall region defect isolations(a1)–(a4) representing one normal and three defective images of foreign matter, bubble, and cords break;(b1)–(b4) corresponding reconstructed images based on ITPCR with k=3; and (c1)–(c4) corresponding binarized images

3.3 Tests on crown region defect isolation

(1) New question risen in binarization threshold choice

Fig.7 (a1)–(a3) display one normalcrown region and two defective crown regions of tireX-ray images. Fig.7 (b1)–(b3) display the corresponding reconstructed images based on ITPCRwith k=3. Binarization threshold of c=4.5 obtained in 3.2 section for sidewall region image is not apt for crown region, for their pixel bool values of Fig.7 (b1)–(b3) are all set to 255, where all information are wipped off, so there are a bit difference for binarizations in crown region defect detections as below.

(2) Special steps for crown regiog defetct isolation

We adopt 2 times binarization operations respectively, for the first time binarization for Fig.7 (b1)–(b3) we learn

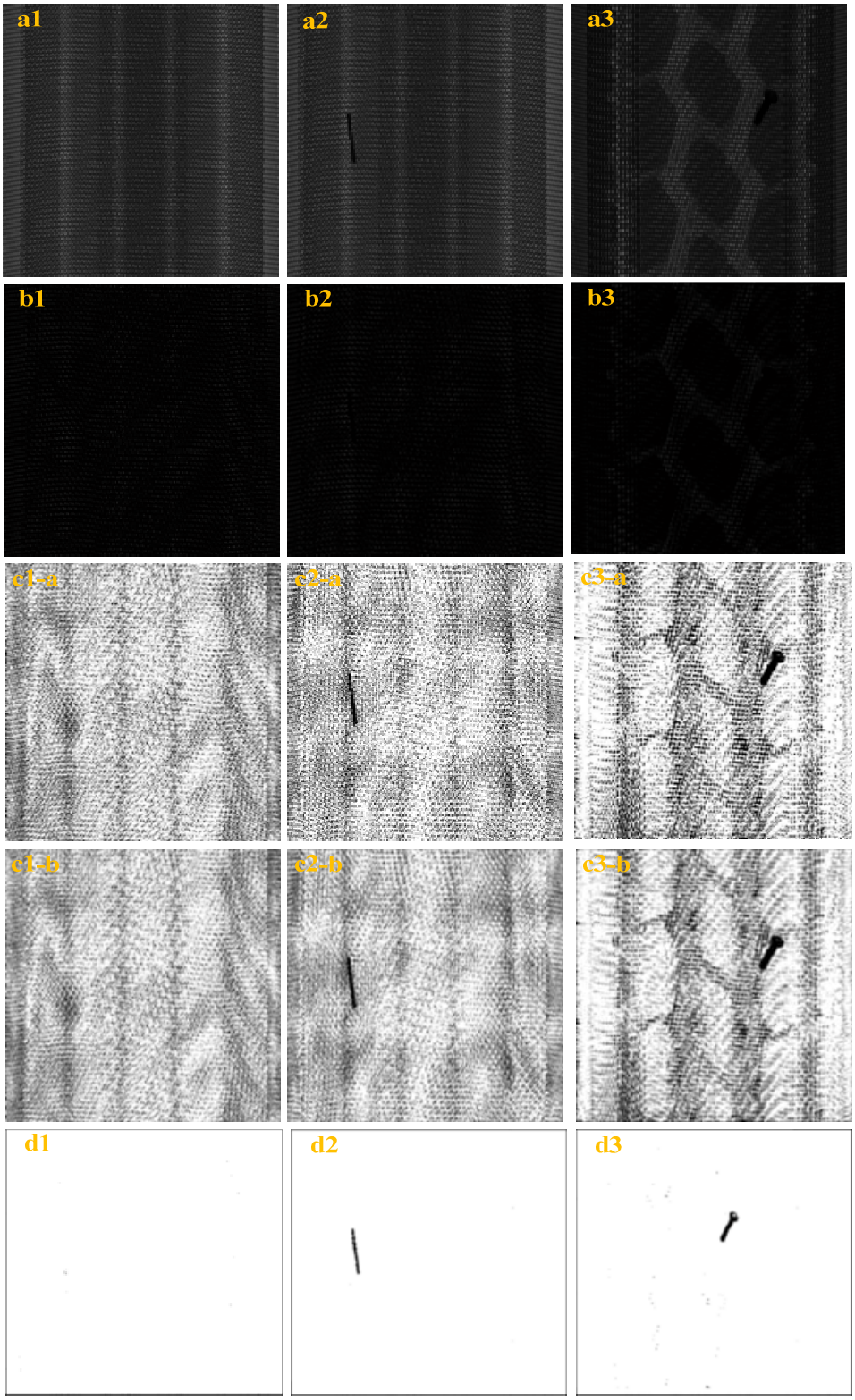

Fig. 7 a1–a3 One defect-free tire crown X-ray images and two defective images with foreign matters affiliation to different types of tires ; b1–b3 corresponding the truncation error images; c1–c3 corresponding filtered binarized images ;and d1–d3 corresponding binarized images which is again the binarization result.

the statistical value of parameter c is 1.0, their results are demonstrated in Fig.7 (c1a)–(c3a), they are quite different from sidewall regions where rich high frequency textures are contained. Before the second time binarization for Fig.7 (c1a)–(c3a), we adopt a 5 by 5 mean filtering method with filter weights of 1/25, their filtering results are shown in Fig.7 (c1b)–(c3b), where high frequency noise are removed away. Fig.7 (d1)–(d3) are results of the second binarizations using the statistically process controlled threshold of c= 3.5. As can be seen, Fig.7 (d1) does not show any defects and noises, and Fig.7 (d2)–(d3) only display clearly the defects. Further more, our proposed scheme revealed the defect location as well as given roughly defect shape. The defect shape can also provide geometrical features such as area, centroid, perimeter, major (minor) axis or elongation to identify the defect by comparing to the specification, or to identify the type of defect according to discriminating features to a classifier.

4. CONCLUSIONS AND ANALYSES

In an automatic tire defect inspection system, we often detectthe problem of some small patches of defects in tire X images, e.g., the foreign matter defect, the bubble defect, cords break.Our proposed methodis different from the widely used methods at which itdoes not need textural features extraction from every tire X-ray image and perform defects matching. Our innovation is to use PCA method in a different way which is to make use of the residual of principal components, furthermore we test the optimum values for k major components and binarization threshold parameter c which are statistically accurate for these similar defects isolations for tire X ray images.Additionallyour methodcan either reveal the defect location or given roughly defect shape so that the tires can be repaired and defects can be identified.However, this method may not suitableto deal with too large-sized defectswhich severely damage the regularity nature texture of tire,which is a subject to be further researched.

REFERENCES

[1] A. Kumar, “Computer-vision-based fabric defect detection: a survey,”IEEE Trans. Industrial Electronics , vol. 55, no.1, pp.348–363, 2008.

[2] Y. ZHANG. “research on nondestructive tire defect detection using computer vision methods[D],” qingdao university of science and technology, pp.1-6, 2014.

[3] A.Kumar (2008) Computer-vision-based fabric defect detection: asurvey. IEEE Trans Ind Electron 55(1):348–363

[4] Q. Guo and Z. Wei, “Tire defect detection using image componentdecomposition,” Research Journal of Applied Sciences, Engineeringand Technology, vol. 4, no. 1, pp.41–44, 2012.

[5] J. Zhou and J. Wang, “Fabric defect detection using adaptive dictionaries,” Textile Research Journal, vol. 83, no. 17, pp.1846–1859, 2013.

[6] W. Zhou, M. Fei, H. Zhou and K. Li, ”A sparse representation basedfast detection method for surface defect detection of bottle caps,”Neurocomputing,Vol. 123, Issue 1, 404-414, 2014.

[7] Y. Xiang, C. Zhang, Q. Guo. A dictionary-based method for tire defect detection[C]// Information and Automation (ICIA), 2014 IEEE International Conference on. IEEE, pp.519-532, 2014

[8] Lu CJ, Tsai DM (2008) Independent component analysis-baseddefect detection in patterned liquid crystal display surfaces. ImageVis Comput 26:955–970

[9] X. Zhang, H. Sun, Y. Zhou, et al. A Novel Method for Surface Defect Detection of Photovoltaic Module Based on Independent Component Analysis[J]. Mathematical Problems in Engineering, 2013, 112(2013):147-160.

[10] Jayanta K. Chandra & Asit K. Datta (2013) Detection of defects in fabricsusing subimage-based singular value decomposition, The Journal of The Textile Institute, 104:3,295-304, DOI: 10.1080/00405000.2012.721206

[11] Lu CJ, Tsai DM (2005) Automatic defect inspection for LCDsusing singular value decomposition. Int J Adv Manuf Technol25:53–61

[12] Perng DB, Chen SH, Chang YS (2010) A novel internal threaddefect auto-inspection system. Int J Adv Manuf Technol 47(5–8):731–743

[13] Tsai DM, Chiang CH (2003) Automatic band selection forwavelet reconstruction in the application of defect detection.Image Vis Comput 21(5):413–431

[14] C H. Hu, H P. Liang. Wood surface texture inspection using automatic selection band for wavelet reconstruction[C]// Society of Photo-Optical Instrumentation Engineers (SPIE) Conference Series. Society of Photo-Optical Instrumentation Engineers (SPIE) Conference Series, 2008.

[15] Jolliffe I.T. Principal Component Analysis, Series: Springer Series in Statistics, 2nd ed., Springer, NY, 2002, XXIX, 487 p. 28 illus. ISBN 978-0-387-95442-4

[16] A. Ranade, SS. Mahabalarao, S. Kale (2007) A variation on SVDbased image compression. Image Vis Comput 25:771–777